

Three-Wave Resonance Grazing Incidence X-Ray Diffraction: A Novel Method for Direct Phase Determination of Surface In-Plane Reflections

Shih-Lin Chang,^{1,2} Yi-Shan Huang,¹ Chun-Hsiung Chao,¹ Mau-Tsu Tang,² and Yuri P. Stetsko³

¹Department of Physics, National Tsing Hua University, Hsinchu, Taiwan, Republic of China 300

²Synchrotron Radiation Research Center, Hsinchu, Taiwan, Republic of China 300

³Chernovtsy State University, Chernovtsy 274012, Ukraine

(Received 4 August 1997)

Three-wave resonance grazing incidence x-ray diffraction is realized for the first time by tuning the x-ray photon energy to match the incident wave vector with the coplanar momentum transfers of crystal surface in-plane reflections. Near the resonance energy, the observed specularly diffracted intensities decreasing at lower energies and increasing at higher energies or vice versa reveal the effects of reflection phases due to the coherent interaction of x-ray surface waves. This experiment thus provides a new way of direct phase determination for surface in-plane reflections. [S0031-9007(97)05055-2]

PACS numbers: 61.10.Dp, 61.10.Eq, 61.10.Kw

The x-ray phase problem is a long-standing physically unsolved important problem in x-ray optics, diffraction physics, and crystallography, because the phase of a scattered radiation like x rays cannot be determined from intensity measurement of a simple reflection and the phases of the structure factors involved in x-ray diffraction experiments play a decisive role in determining the relative positions of atoms in a crystal unit cell [1]. Although the existing mathematical methods using a large collection of diffraction-intensity data [1] and the multiple diffraction techniques utilizing interference effects [2–13] could provide solutions to this problem for bulk crystals, the x-ray phase problem still exists, especially for cases involving surfaces and interfaces. Until now, phases of reflections from surfaces/interfaces have been determined mainly by structure modeling via intensity matching or by Patterson methods on a trial and error basis [14]. Direct physical measurements of phases from surface related reflections have not so far been reported in the literature. In this Letter, we concentrate on surface in-plane reflections of a thin crystal plate and realize three-wave grazing incidence x-ray diffraction (GIXD) for these surface in-plane reflections at a resonance x-ray photon energy. From the variation of specularly diffracted intensity distribution versus photon energies, resulting from the coherent dynamical interaction of x-ray surface waves, we demonstrate the first direct phase determination of crystal surface in-plane reflections. A general way of determining phases of surface in-plane reflections from three-wave resonance GIXD for centrosymmetric crystals is also presented.

Three-wave GIXD takes place when two sets of atomic planes G and L perpendicular to the crystal surface are simultaneously brought into position to diffract a grazing incident beam O . Namely, in reciprocal space, the reciprocal lattice points (rlp's) O , G , and L lie in the equatorial circle of the Ewald sphere parallel to the crystal surface, where O stands also for the incident reflection. Since the radius of the circle is

$1/\lambda$, λ being the x-ray wavelength used, three-wave GIXD can only occur at a specific λ_M (photon energy E_M) [see Fig. 1(a)] [15]. Because of the grazing incidence geometry [Fig. 1(b)] and the involved surface in-plane reflections G and L , the specularly diffracted waves of the two surface reflections have appreciable intensities which can be detected experimentally. When a three-wave (O , G , and L) GIXD occurs at the photon energy E_M , one of the surface specularly diffracted waves, G or L , can be treated as a reference for the other wave. The interaction of the G and L diffracted wave via the coupling $G - L$ reflection within the crystal gives rise to intensity modification on the reference wave. This modification is, thus, related to the phases of G , L , and $G - L$ reflections or more precisely, the triplet phase δ_3 of the structure-factor triplet $F_{-G}F_LF_{G-L}$. When the photon energies $E \neq E_M$, the G or L reflection becomes a simple two-wave reflection. We, therefore, see only the reference wave at a corresponding Bragg angle. This consideration for the grazing incidence geometry is the basis of this investigation for phase determination.

The case studied is the three-wave GIXD [$O(000)$, $G(440)$, and $L(404)$] of a $(\bar{1}11)$ cut silicon crystal, where the in-plane reflections (440) and (404) are parallel to the $(\bar{1}11)$ plane. As shown in Fig. 1(a), this three-wave GIXD takes place when the three reciprocal lattice points O , G , and L lying in the crystal surface are on the reflection circle of the Ewald sphere, with the radius CO equal to $1/\lambda_M = a_{440}^*/(2 \cos 30^\circ)$, where a_{440}^* is the reciprocal lattice vector of the (440). For this three-wave GIXD, λ_M is 1.66286 Å, namely $E_M = 7.46613$ keV. The incident and the diffracted waves are along the wave vectors \vec{K} 's as shown. To monitor the diffracted intensities of this in-plane three-wave reflection, only the surface specularly diffracted intensities of (440) and (404) are measured.

The experiments were carried out with the wiggler beam line SB-05 at the Synchrotron Radiation Research

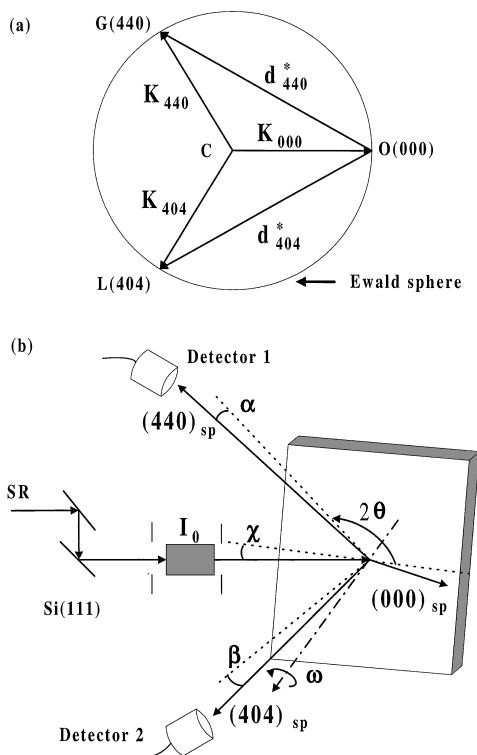


FIG. 1. (a) Geometry of three-wave (000)(440)(404) GIXD of Si in reciprocal space for $E = E_M$: The \vec{K} 's are the wave vectors of the diffracted waves. (b) Experimental setup: Only the specularly reflected waves, $(440)_{sp}$ and $(404)_{sp}$, were detected for phase analysis. α , β , and χ are the tilt angles from the crystal surface. The ω axis is along the $[\bar{1}11]$.

Center (SRRC). The σ -polarized incident beam from the 1.86 tesla 25-pole wiggler with the magnet gap 22 mm was focused and monochromatized by a sagittal Si(111) double-crystal monochromator (SDCM), when the SRRC storage ring was operating at 1.5 GeV and 200 mA. The σ -polarization vector was perpendicular to the crystal surface along the $[\bar{1}11]$ direction. A 1 m evacuated beam path with two sets of slits on both ends was used. An ion chamber acting as the incident beam monitor I_0 was placed in the middle of the beam path [Fig. 1(b)]. A 1 mm thick $(\bar{1}11)$ cut silicon thin plate, with the large area $20 \times 20 \text{ mm}^2$ parallel to the $(\bar{1}11)$ plane, was mounted on an 8-circle Huber diffractometer. Slits and two-scintillation counters were used to monitor the (440) and (404) reflections. The distances from the wiggler to the SDCM and from the SDCM to the crystal were 24 and 5.5 m, respectively. The beam divergences were 0.02° vertical and 0.03° horizontal. The energy resolution of the SDCM was 2 eV [16]. The photon energy was first set to E_M . The crystal was aligned in such a way that the incident beam at the angle of incidence $\chi = 0.18^\circ$ was diffracted into the two detectors placed at $2\theta = 120^\circ$ and -120° and the scattering angles $\alpha = \beta = 0.4^\circ$ [see Fig. 1(b)]. The crystal surface roughness measured from

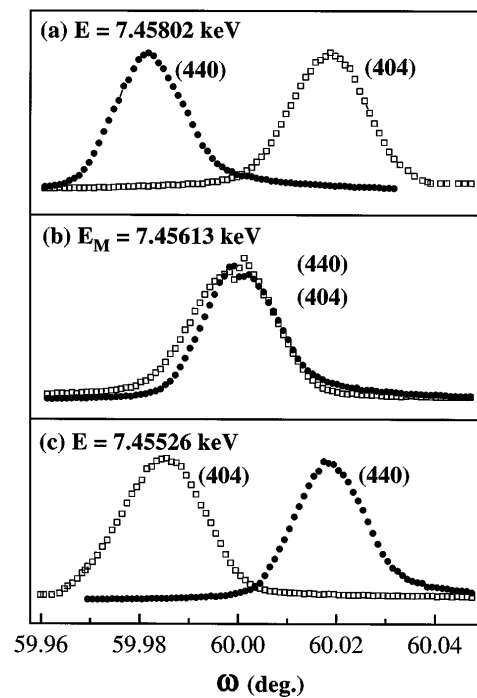


FIG. 2. Rocking curves of the specularly reflected (440) and (404) during the photon-energy scans at the nominal energies (a) 7.45 802 keV, (b) $E_M = 7.45 613$ keV, and (c) 7.45 526 keV. In (b), the three-wave GIXD occurs.

reflectivity was about 10 \AA and the critical angle θ_c measured for external total reflection was $\chi = 0.18^\circ$. The surface miscut was negligibly small. To achieve an energy resolution better than 2 eV for photon-energy scans, one-way rotation of the SDCM at 0.2 eV/step was carried out to suppress gear backlash. During an energy scan for the three-wave geometry, at each energy step (channel), the crystal was rotated around $[\bar{1}11]$, the ω scan, and the corresponding rocking curves of the (440) and (404) were recorded [Fig. 2(a)]. The angular separation of the peaks between the two rocking curves provided an additional energy calibration of the incident photons. When the two rocking curves overlapped with each other, i.e., at the same Bragg angle, the three-wave GIXD was ensured to occur [Fig. 2(b)]. The integrated intensities of the surface specularly diffracted (440) and (404) versus the photon energies are plotted in Figs. 3(a) and 3(b), respectively. The asymmetry of the intensity distributions is clearly visible.

We then carried out theoretical calculations based on Ref. [17] to analyze the relation between the intensity asymmetry and the triplet phases, using the dynamical theory for GIXD [15,17–20]. The calculated specularly diffracted intensities of the (440) and (404) for the triplet phases $\delta_3 = \delta(440) + \delta(404) + \delta(04\bar{4}) = 0^\circ$ and 180° are shown also in Fig. 3. (Note that, since silicon involves a center of inversion, the phases of the reflections are either 0° or 180° .) The structure-factor moduli, 113.80

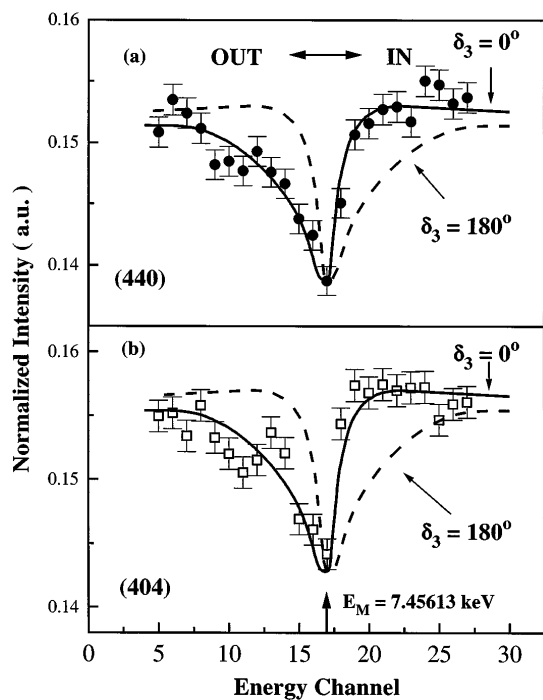


FIG. 3. Surface specularly diffracted integrated intensities of (a) (440) and (b) (404) versus energy channel (1 channel = 0.2 eV). The solid curve is calculated for $\delta_3 = 0^\circ$ and the dashed curve for $\delta_3 = 180^\circ$. The IN and OUT situations are also indicated.

electrons for (000) and 44.82 electrons for (440), (404), and (044), with a proper temperature factor were used in the calculation. From Fig. 3, the asymmetry of the calculated curve for $\delta_3 = 180^\circ$ is reversed as compared with that for $\delta_3 = 0^\circ$. The well-fit experimental data to the calculated curve for 0° indicates that the δ_3 for this three-wave in-plane reflection is 0° .

The origin of this phase dependent intensity distribution can be understood from the dispersion surfaces calculated for $\delta_3 = 0^\circ$ and 180° at $\chi = \theta_c$ (Fig. 4). The dispersion surface describes the relationship between the real parts of the components K_z^r of the diffracted wave vectors normal to the crystal surface and the photon energy, just like the momentum versus energy for the electronic band structures in solids. For this three-wave GIXD, branches 2 and 3 of the dispersion surface are most effective. The closer the dispersion branches, the stronger the diffracted intensity [21]. For $\delta_3 = 0^\circ$, branches 2 and 3 are very close to each other for $\Delta E = E - E_M$ slightly greater than zero [Fig. 4(a)], while for $\delta_3 = 180^\circ$, these two branches are far apart and the closest position between the two is around $\Delta E \cong -0.02$ eV. These explain why the asymmetry of the intensity distribution shown in Fig. 3 depends on the phase δ_3 .

According to the dynamical theory, the specularly diffracted intensities of a three-wave GIXD result from the interference between the two-wave specular reflec-

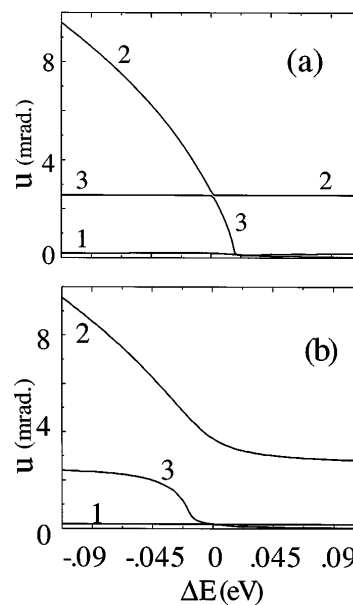


FIG. 4. Sections of the dispersion surfaces ($u = K_z^r/k$ versus ΔE) at $\chi = \theta_c$ for the three-wave GIXD studied with (a) $\delta_3 = 0^\circ$ and (b) $\delta_3 = 180^\circ$. (K_z^r is the real part of the normal component of the wave vector K and $k = 1/\lambda$.)

tion G and the specularly “detoured” diffraction via the L reflection and the $G - L$ coupling reflection. The resultant phase δ_R of the specularly diffracted reflection measured is, therefore, the sum of the phase δ_P due to the beam polarization, the triplet phase δ_3 of the $-G$, L , and $G - L$ reflections, and the phase δ_D due to the three-wave diffraction geometry, namely, $\delta_R = \delta_P + \delta_D + \delta_3$. $\delta_P = 0^\circ$ for a σ -polarized beam. For π polarization, $\delta_P = 0^\circ$ or 180° , depending on whether the polarization factor $\cos 2\theta_G$ is positive or negative, θ_G being the Bragg angle of the G reflection. The geometry phase δ_D is 0° for an IN and 180° for an OUT situation. More specifically, if the scan is from low to high energies, δ_D is related to the relative positions of the rlp’s G and L with respect to the reflection circle of the Ewald sphere during the photon-energy scan, i.e., the relative motion of the rlp towards (IN) or out of (OUT) the Ewald sphere δ_D is 0° for $\vec{g} \cdot \vec{l} - l^2 > 0$ and 180° for $\vec{g} \cdot \vec{l} - l^2 < 0$, where \vec{g} and \vec{l} are the reciprocal lattice vectors of the G and L reflections. From the dynamical analysis and calculations, experimental phase determination (the sign of $\cos \delta_3$) for surface in-plane reflections of centrosymmetric crystals like Si can be deduced as

$$S(\cos \delta_3) = S_P(\cos \delta_P) \cdot S_D(\cos \delta_D) \cdot S_L. \quad (1)$$

Namely, the sign $S(\cos \delta_3)$ of $\cos \delta_3$ can be determined from the sign of $\cos \delta_P$, the sign of $\cos \delta_D$, and the sign S_L of the asymmetry of the intensity line profile measured from the energy scan. S_L is positive if the intensity first decreases at lower photon energies and then increases at

higher energies when crossing the energy E_M , and S_L is negative for the reversed asymmetry.

We have verified this sign relation experimentally by rotating the crystal 90° about the incident beam so the beam was π polarized. The reversal of intensity asymmetry of energy scans was detected (not shown). Similarly, the effect of the IN-OUT geometry on the intensity asymmetry were also observed. The dynamical calculation also confirmed this sign relation. Detailed calculations will be reported elsewhere. Interestingly, the phase relation of three-wave GIXDs [Eq. (1)] deduced from photon-energy scans is exactly the same as of the usual (wide-angle) three-wave diffraction in crystal bulk from angle (momentum) scans [6,8,13]. However, it should be noted that to maintain the grazing incidence geometry for surface in-plane reflections and the phase sensitivity for diffracted intensities, it is a must to use energy scans for the present purposes.

We have also estimated from the dynamical calculation the penetration depth l_p of x-rays in the sample. l_p ranges from 0 to 300 \AA , depending on the incident angle $0 < \chi < \theta_c$. $l_p \equiv 300 \text{ \AA}$ at $\chi = \theta_c$. The depth sensitivity of the three-wave GIXD is very similar to the usual two-wave GIXD. Since the determined $\delta_3 = \delta(\bar{4}\bar{4}0) + \delta(404) + \delta(0\bar{4}\bar{4}) = 0^\circ$ for the present experiment, and since $\delta(\bar{4}\bar{4}0) = \delta(404) = \delta(0\bar{4}\bar{4})$ from the space group F_{d3m} for Si, therefore, the phases δ of these reflections are all equal to zero.

In conclusion, we have realized a three-wave resonance GIXD by tuning the x-ray photon energy across a three-wave GIXD diffraction position and demonstrated the first successful direct phase determination for crystal surface in-plane reflections. A simple and general sign relation is also deduced for direct experimental phase determination. Since the tunability of photon energy of synchrotron radiation facilitates the occurrence of three-wave and four-wave GIXD for any two or three in-plane reflections, the present method is applicable to phasing in-plane reflections of crystals, where coherent interaction is retained. For example, for crystals having two- or four-fold symmetry, four-wave GIXD can be useful and, for samples with three- or six-fold symmetry, three-wave GIXDs are practical for the phasing experiments.

The authors are indebted to the National Science Council for financial support. Y.S.H. and C.H.C acknowledge the same organization for providing graduate fellowships during the course of this study.

-
- [1] See, for example, H.A. Hauptman, *Phys. Today* **42**, No. 11, 24 (1989).
 - [2] M. Hart and A.R. Lang, *Phys. Rev. Lett.* **7**, 120 (1961).
 - [3] R. Colella, *Acta Crystallogr. Sect. A* **30**, 413 (1974).
 - [4] B. Post, *Phys. Rev. Lett.* **39**, 760 (1977).
 - [5] L.D. Chapman, D.R. Yoder, and R. Colella, *Phys. Rev. Lett.* **46**, 1578 (1981).
 - [6] S.L. Chang, *Phys. Rev. Lett.* **48**, 163 (1982).
 - [7] H.J. Juretschke, *Phys. Rev. Lett.* **48**, 1487 (1982); *Phys. Lett.* **92A**, 183 (1982).
 - [8] Q. Shen and R. Colella, *Acta Crystallogr. Sect. A* **44**, 17 (1988).
 - [9] S.L. Chang and M.T. Tang, *Acta Crystallogr. Sect. A* **44**, 1065 (1988).
 - [10] Q. Shen and K.D. Finkelstein, *Phys. Rev. Lett.* **65**, 3337 (1990).
 - [11] K. Hümmer, E. Weckert, and H. Bondza, *Acta Crystallogr. Sect. A* **45**, 182 (1989); **46**, 393 (1990); **47**, 60 (1991).
 - [12] S.L. Chang, H.E. King, M.T. Huang, and Y. Gao, *Phys. Rev. Lett.* **67**, 3113 (1991).
 - [13] E. Weckert and K. Hümmer, *Acta Crystallogr. Sect. A* **53**, 108 (1997), and the references therein.
 - [14] For reviews, see I.K. Robinson and D.J. Tweet, *Rep. Prog. Phys.* **55**, 599 (1992); S. Dietrich and A. Haase, *Phys. Rep.* **260**, 1 (1995), and references therein.
 - [15] H.H. Hung and S.L. Chang, *Acta Crystallogr. Sect. A* **45**, 823 (1989).
 - [16] K.L. Tsang *et al.*, *Rev. Sci. Instrum.* **66**, 1812 (1995).
 - [17] Yu. P. Stetsko and S.L. Chang, *Acta Crystallogr. Sect. A* **53**, 28 (1997).
 - [18] T.P. Tseng and S.L. Chang, *Acta Crystallogr. Sect. A* **46**, 567 (1990).
 - [19] A.M. Afanasiev and M.K. Melkonyan, *Acta Crystallogr. Sect. A* **39**, 207 (1983).
 - [20] S.M. Durbin and T. Gog, *Acta Crystallogr. Sect. A* **45**, 132 (1989).
 - [21] P.P. Ewald and Y. Heno, *Acta Crystallogr. Sect. A* **24**, 5 (1968).